Supporting Information

A stable and flexible HOF@SA membrane for efficient adsorption of organic cationic dyes

Ruiqi Zhu,[a] Qiuxia Wu,[a] Shengjie Lin,[a] Limin Wang,[a] Ye Liang,[a] Lin Zhang,[a] Dian Zhao,[a] Yabing He*[a] and Banglin Chen*[ab]*

[a]Key Laboratory of the Ministry of Education for Advanced Catalysis Materials, College of Chemistry and Materials Science, Zhejiang Normal University, Jinhua 321004, China. Email: linzhang@zjnu.edu.cn (L. Zhang); heyabing@zjnu.cn (Y. He).

[b]Fujian Provincial Key Laboratory of Polymer Materials, College of Chemistry & Materials Science, Fujian Normal University, Fuzhou 350007, P.R. China. Email: banglin.chen@fjnu.edu.cn (B. Chen).

1. Experimental Section/Methods

Preparation of HOF-NBDA.

The preparation of HOF-NBDA in this study was based on the method described in the literature with some modifications[1]. 10 mg 4',4'',4'''-nitrilotribiphenyl-3,5-dicarboxylic acid (NBDA) and 1 ml DMF were added into a 20 ml glass bottle. After sonication until dissolved, 4 ml anhydrous ethanol was added. The mixture was left to evaporate at room temperature for 3 days. The resulting crystals were washed with ethanol and then dried at 60 °C for 6 hours.

Preparation of SA hydrogel and HOF-NBDA@SA.

The preparation of a single sodium alginate (SA) hydrogel film and HOF-NBDA@SA hydrogel film in this article referred to the methods in the literature with some modifications[2]. 50 mg SA was dissolved in 2.5 ml deionized water to prepare the SA solution, and 510 mg sodium alginate solution (containing 10 mg of SA) was transferred onto a glass slide and scraped into a thin film with a 750 nm scraper. The glass slide was rapidly placed in a 1.5 wt% calcium chloride solution, and then washed repeatedly with deionized water to remove free calcium ions, resulting in the formation of the SA hydrogel. HOF-NBDA@SA was prepared similarly to SA hydrogels, except that 50 mg of HOF-NBDA was added to the prepared solution, and the mixture was stirred thoroughly to ensure uniform distribution of the HOF powder. 520 mg of the mixture (containing 10 mg SA, 10 mg HOF-NBDA and 500 mg H_2O) was then weighed to make a thin membrane with the weight ratio of HOF-NBDA to SA being 1:1. The HOF-NBDA@SA of this ratio was taken as the main investigated sample in this work. Then HOF-NBDA@SA membranes (containing 500 mg H_2O) with different HOF-NBDA/SA weight ratio of 1:2, 3:2, 2:1 were respectively prepared based on the similar methods.

Materials and Characterizations.

Methylene Blue (MB) and Acid Orange G (AOG) were purchased from Shanghai Bior Chemical Reagent Co., Ltd., Methyl Violet (MV) from Shanghai Aladdin Bio-Chem Technology Co., Ltd., 4-Di-1-ASP (DSM) and Basic Blue 3 (BB-3) from Tianjin Xienshi Biochemical Technology Co., Ltd., Pyronine B (PB) from Acros Organics, Congo red (CR) from Sann Chemical Technology (Shanghai) Co., Ltd., Methyl Orange (MO) and Sunset Yellow (SY) from Shanghai Yien Chemical Technology Co., Ltd., Eosin Y (EY) and sodium alginate from Shanghai Mayer Biochemical Technology Co., Ltd., N, N-dimethylformamide (DMF, >99.5%) from Shanghai Lingfeng Chemical Reagent Co., Ltd., methanol (AR, >99.5%) and anhydrous ethanol (AR, >99.7%) as well as calcium chloride (AR) from Shanghai Lianshi Chemical Reagent Co., Ltd., hydrochloric acid (AR) from China Pharmaceutical Group Chemical Reagent Co., Ltd., and 4',4'',4'''-nitrilotribiphenyl-3,5-dicarboxylic acid from Nanjing AIM Materials Technology Co., Ltd. The reagents and chemicals used in this study were used directly without further treatment after commercial purchase.

Nitrogen adsorption data were obtained from measurements using a fully automated gas adsorption meter (Micromeritics ASAP 2020HD88) by a liquid nitrogen bath and a circulating thermostatic water bath (Julabo F12) with temperature control at 77K. Prior to nitrogen isotherm testing, samples were solvent exchanged with anhydrous ethanol and activated by vacuum drying at 373K for 10 h. The morphology of the cross section of HOF@SA was characterized by Hitachi S-4800 field emission scanning electron microscope (SEM) after undergoing liquid nitrogen cleavage and freeze drying. Powder X-ray diffraction (PXRD) data of the samples were collected on a D8 Advance X-ray powder diffractometer using a Cu Kα (λ = 1.5418 Å, U = 40 kV, I = 40 mA) beam with a scanning speed of 5 °·min^{-1} and 2θ range of 3-45 °. To test the water and acid-base stability of HOF-NBDA, 10 mg HOF-NBDA was immersed in 20 ml aqueous solution with pH ranging from 1 to 11 for 7 days and then centrifuged and dried as a sample for testing. In the wavelength range of 400-4000 cm^{-1}, Fourier transform infrared (FTIR) spectra of the synthetic ligands and corresponding crystals were obtained using the Nicolet 5DX FTIR infrared spectrometer with the potassium bromide pellet method. The Zeta potential analysis was performed using the Zetasizer Nano ZS90 analyzer from Malvern Instruments. 1 mg HOF-NBDA or HOF-NBDA@SA was dispersed in 15 ml of water, sonicated for 3 minutes, and the suspension pH was adjusted by using HCl and NaOH. The Zeta potential of the material suspension at different pH was tested at room temperature. Thermogravimetric analysis (TGA) was conducted using the Netzsch STA F5 thermal analyzer under a nitrogen atmosphere to collect thermogravimetric data. The UV-Vis absorbance spectra were obtained from a Hitachi UH5300 UV-Visible spectrophotometer with a scanning speed of 400 nm/min and a scanning range of 300-800 nm.

Adsorption selectivity.

20 ml aqueous solutions (10 ppm) of DSM, MB, PB, MV, BB-3 cationic dyes, as well as MO, EY, SY, CR, AOG anionic dyes were prepared separately. 10 mg HOF-NBDA adsorbent was dispersed in each solution, and the total contact time between HOF and dye solution is kept in 10 minutes. The absorbance of DSM, MB, PB, MV, BB-3, MO, EY, SY, CR, AOG before and after adsorption by the adsorbent was measured using a UV-Visible spectrophotometer. Mixtures of 20 mL BB-3&AOG, DSM&EY, MV&SY, and MB&MO solutions (10 ppm) were prepared, and 10 mg HOF-NBDA adsorbent was added into each mixed solution. Following the above procedure, the selective adsorption of the 10 mg adsorbent for the mixed binary systems of cationic and anionic dyes was tested.

Dynamic adsorption experiments were conducted on the binary systems of the above-mentioned cationic and anionic mixed dyes. The membrane was immersed in these dye solutions for 0, 10, 60, 70, 80, 90, 120, 150, 180, 210 minutes, and UV-Vis absorption spectra were measured.

Adsorption kinetics.

The present study focused on the adsorption kinetics of 10 mg HOF-NBDA and 510 mg SA membranes (containing 10 mg SA and 500 mg H_2O) and HOF-NBDA@SA membranes (containing 500 mg H_2O) with HOF-NBDA/SA weight ratios of 1:2, 1:1, 3:2, 2:1, and 5:2 for adsorption of 20 ml MB aqueous cationic dye solution (10 ppm). The powder was evenly mixed and then placed on a fixed rack for static adsorption. At different time points, the adsorbents in the suspension were centrifuged out from the MB solution, and the absorbance of the MB solution was measured by using UV-Vis spectrophotometry to obtain the concentration (C_t, mg·L^{-1}).

The adsorption amount (Q_t, mg·g^{-1}) of MB at time (t, min) can be calculated according to:

$$Q_t = \left(C_0 - C_t\right) \times \frac{V}{M} \#(1)$$

where C_0 (mg·L^{-1}) is the initial concentration of MB in the aqueous solution, V (L) is the volume of the solution; M (mg) is the weight of the adsorbent.

The adsorption kinetics experimental data can be fitted by nonlinear pseudo-first-order (PFO) or pseudo-second-order (PSO) models：

PFO Model:

$$Q_t = Q_e\left(1 - e^{\left(-k_1 t\right)}\right)\#(2)$$

PSO Model:

$$Q_t = \frac{k_2 t Q_e^2}{1 + tQ_e k_2}\#(3)$$

where Q_e ($mg \cdot g^{-1}$) denotes the adsorption amount at equilibrium, k_1 (min^{-1}) and k_2 ($g \cdot mg^{-1} \cdot min^{-1}$) are the rate constants of the PFO and PSO models, respectively[3, 4].

In order to explore the kinetic diffusion mechanism, the intraparticle diffusion model is used to fit the kinetic data[5].

$$Q_t = k_{i,d} t^{\frac{1}{2}} + C\#(4)$$

where $k_{i,d}$ ($mg \cdot g^{-1}$ $min^{-1/2}$) represents the rate constant, C is a constant for any experiment (mg/g)[6].

Adsorption isotherms

The adsorption isotherm is a concentration curve drawn at a certain temperature when solute molecules are adsorbed at the liquid-solid interface and reach equilibrium. This relationship can be expressed by equations to fit the data and analyze the adsorption process. In an isothermal experiment, 10 mg of HOF-NBDA or 520 mg of HOF-NBDA@SA (containing 10 mg SA, 10 mg HOF-NBDA and 500 mg H_2O) is added to a solution of 20 ml MB at different concentrations (5 ppm-1250 ppm). In this work, the effect of HOF-NBDA@SA membranes with different doping ratios on adsorption was investigated. These membranes were immersed in 20 ml MB solution (1250 ppm) and tested for equilibrium adsorption. The adsorption experiment is conducted at 30 °C in a constant temperature water bath. To reach adsorption equilibrium, the experiment was soaked for up to 7 days. Different adsorption isotherm models (Langmuir model[7], Freundlich model[8], and Sips model[9]) were used to fit the adsorption process of the adsorbent for MB molecules:

Langmuir Model:

$$Q_e = \frac{Q_m K_l C_e}{1 + K_l C_e}\#(5)$$

Freundlich Model:

$$Q_e = K_f C_e^{\frac{1}{n}}\#(6)$$

Sips Model:

$$Q_e = \frac{Q_m\left(K_s C_e\right)^n}{1 + \left(K_s C_e\right)^n}\#(7)$$

where K_l ($L \cdot mg^{-1}$), K_f ($mg^{1-1/n} \cdot L^{1/n} \cdot g^{-1}$), and K_s ($mg^{1-1/n} \cdot L^{1/n}$) represent the Langmuir constant, Freundlich constant, and Sips constant, respectively. Q_m ($mg \cdot g^{-1}$) is the adsorption capacity, and n is the heterogeneity factor.

The experiments such as adsorption covered in this article are the result of taking the average of several parallel tests.

Reusability

The reusability of adsorbents is a highly-attractive and practical feature in the context of real-life production applications. Accordingly, the recycling performance of HOF-NBDA and HOF-NBDA@SA was evaluated in this study. For the cyclic use of HOF-NBDA powder, the dye-loaded adsorbent was dispersed in methanol for desorption within 10 minutes, centrifuged and dried at 60 °C for 3 hours. The resultant powder was used for the next adsorption cycle. As for the cyclic use of HOF-NBDA@SA, it was immersed in methanol overnight, washed with pure water, and then dried for the next adsorption cycle.

2. Supplementary Tables and Figures

Table S1. Parameters for dyes.

abbreviation	Chemical structure	Molecular size (Å^3)	M_r	charge	λ_{max} (nm)
MB	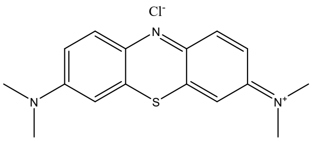	15.81×4.02×7.81	319.85	cationic	664
BB-3	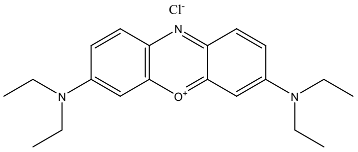	18.43×4.02×9.03	359.89	cationic	654
MV	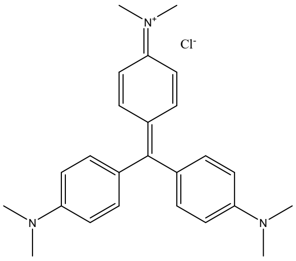	13.92×5.81×15.46	407.99	cationic	578
DSM	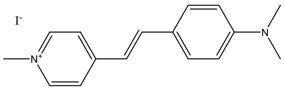	15.94×4.02×7.14	366.24	cationic	450
PB	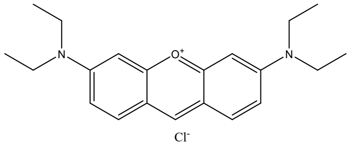	18.43×4.02×9.15	358.91	cationic	546
MO	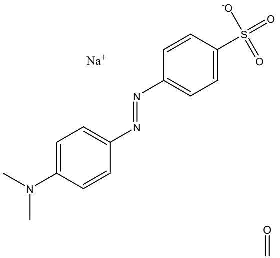	16.40×5.23×7.27	327.33	anionic	464
SY	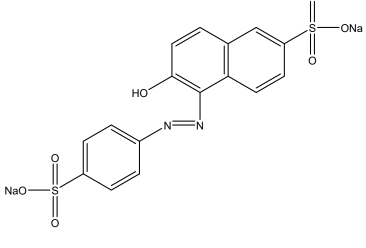	19.77×5.23×12.70	452.36	anionic	482
AOG	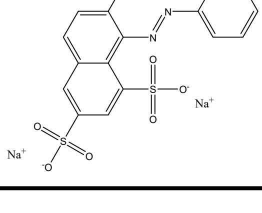	14.75×5.67×10.45	452.36	anionic	478

EY	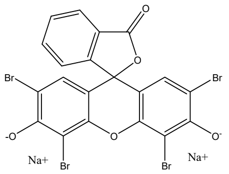	14.20×8.39×11.98	691.85	anionic	516
CR	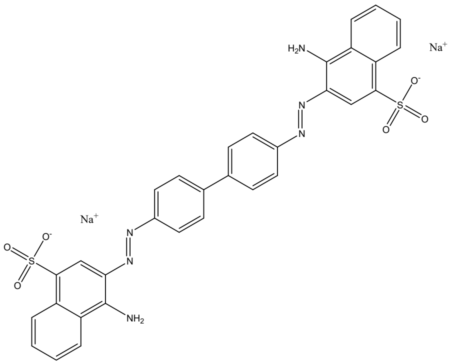	27.02×5.89×10.17	696.66	anionic	500

Table S2. Model parameters of adsorption kinetics of MB and BB-3 adsorption on SA, HOF-NBDA@SA and HOF-NBDA.

	Parameters	SA	HOF-NBDA@SA	HOF-NBDA
MB	PFO			
	Q_e (mg·g^{-1})	10.11	9.491	19.92
	k_1 (min^{-1})	0.0351	0.0439	0.3352
	R^2	0.9802	0.9948	0.9863
	PSO			
	Q_e (mg·g^{-1})	12.77	11.49	20.76
	k_2 (g·mg^{-1}·min^{-1})	0.0026	0.0039	0.0349
	R^2	0.9854	0.9969	0.9678
BB-3	PFO			
	Q_e (mg·g^{-1})	4.248	10.04	19.86
	k_1 (min^{-1})	0.0247	0.0337	0.3158
	R^2	0.9680	0.9986	0.9892
	PSO			
	Q_e (mg·g^{-1})	5.599	12.73	20.78
	k_2 (g·mg^{-1}·min^{-1})	0.0039	0.0024	0.0310
	R^2	0.9730	0.9936	0.9617

Table S3. Adsorption kinetic modeling parameters for the adsorption of 20 ml MB solution (10 ppm) by HOF-NBDA@SA with different doping ratios.

Parameters	HOF-NBDA:SA	1:2	3:2	2:1	5:2
PFO	Q_e (mg·g^{-1})	11.66	6.936	6.045	5.111
	k_1 (min^{-1})	0.0873	0.1096	0.0994	0.0961
	R^2	0.9699	0.9599	0.9805	0.9695
PSO	Q_e (mg·g^{-1})	13.14	7.709	6.723	5.722
	k_2 (g·mg^{-1}·min^{-1})	0.0079	0.0179	0.0185	0.0204
	R^2	0.9817	0.9655	0.9852	0.9674

Table S4. Model parameters of intragranular diffusion of MB and BB-3 on SA, HOF-NBDA@SA and HOF-NBDA.

	Parameters	SA	HOF-NBDA@SA	HOF-NBDA
MB	k_{i1} (mg·g^{-1}·min$^{1/2}$)	0.4086	0.9201	7.055
	C_1	-0.0681	-0.1031	0.1475
	R^2	0.5058	0.8596	0.9712
	k_{i2} (mg·g^{-1}·min$^{1/2}$)	1.299	1.173	1.128
	C_2	-1.018	-0.1219	15.62
	R^2	0.9074	0.9917	0.7113
	k_{i3} (mg·g^{-1}·min$^{1/2}$)	0.6548	0.3388	0.0073
	C_3	3.023	5.856	19.81
	R^2	0.9663	0.8511	0.0459
BB-3	k_{i1} (mg·g^{-1}·min$^{1/2}$)	0.1952	0.5671	6.997
	C_1	-0.0735	-0.0455	-0.0597
	R^2	0.3639	0.8587	0.9676
	k_{i2} (mg·g^{-1}·min$^{1/2}$)	0.4378	1.228	3.003
	C_2	-0.2786	-0.9702	9.696
	R^2	0.9444	0.9854	0.6226
	k_{i3} (mg·g^{-1}·min$^{1/2}$)	0.1219	0.1012	0.0130
	C_3	2.735	8.679	19.65
	R^2	0.8010	0.8640	0.3688

Table S5. Adsorption isotherm model parameters for adsorbent adsorption of MB dye.

Parameters	SA	HOF-NBDA@SA	HOF-NBDA
Langmuir isotherm			
Q_m (mg·g^{-1})	1184.93	738.18	473.52
K_l (L·mg^{-1})	0.0334	0.0643	1.762
R^2	0.9824	0.9765	0.8658
Freundlich isotherm			
K_f (mg1$^{-1/n}$·L$^{1/n}$·g^{-1})	160.43	217.96	180.87
1/n	0.3232	0.2058	0.1689
R^2	0.8468	0.9308	0.8902
Sips isotherm			
Q_m (mg·g^{-1})	1099.71	730.01	652.05
K_s (mg$^{1-1/n}$·L$^{1/n}$)	0.0430	0.0651	0.0856
n	1.303	1.061	0.3319
R^2	0.9897	0.9721	0.8948

Table S6. Summary table of adsorption of MB dyes by different adsorbents.

Adsorbent	Adsorption capacity (mg/g)	Ref.
MIL-88(Fe) filter	602	10
MOF-74（Zn/Fe）	370	11
Pristine UiO-66	370	12
NH_2-MIL-101 (Al)	762	13
NiT20-400/SA	54	14
MoS_2-140	785	15
Zn-MOF	326	16
Activated lignin-chitosan composite extrudates	36.25	17
Kaolin-based mesoporous silica	652.9	18
CS/OSA/2%Ca^{2+}	20.68	19
HOF-NBDA	594.09	This work
HOF-NBDA@SA	729.21	This work

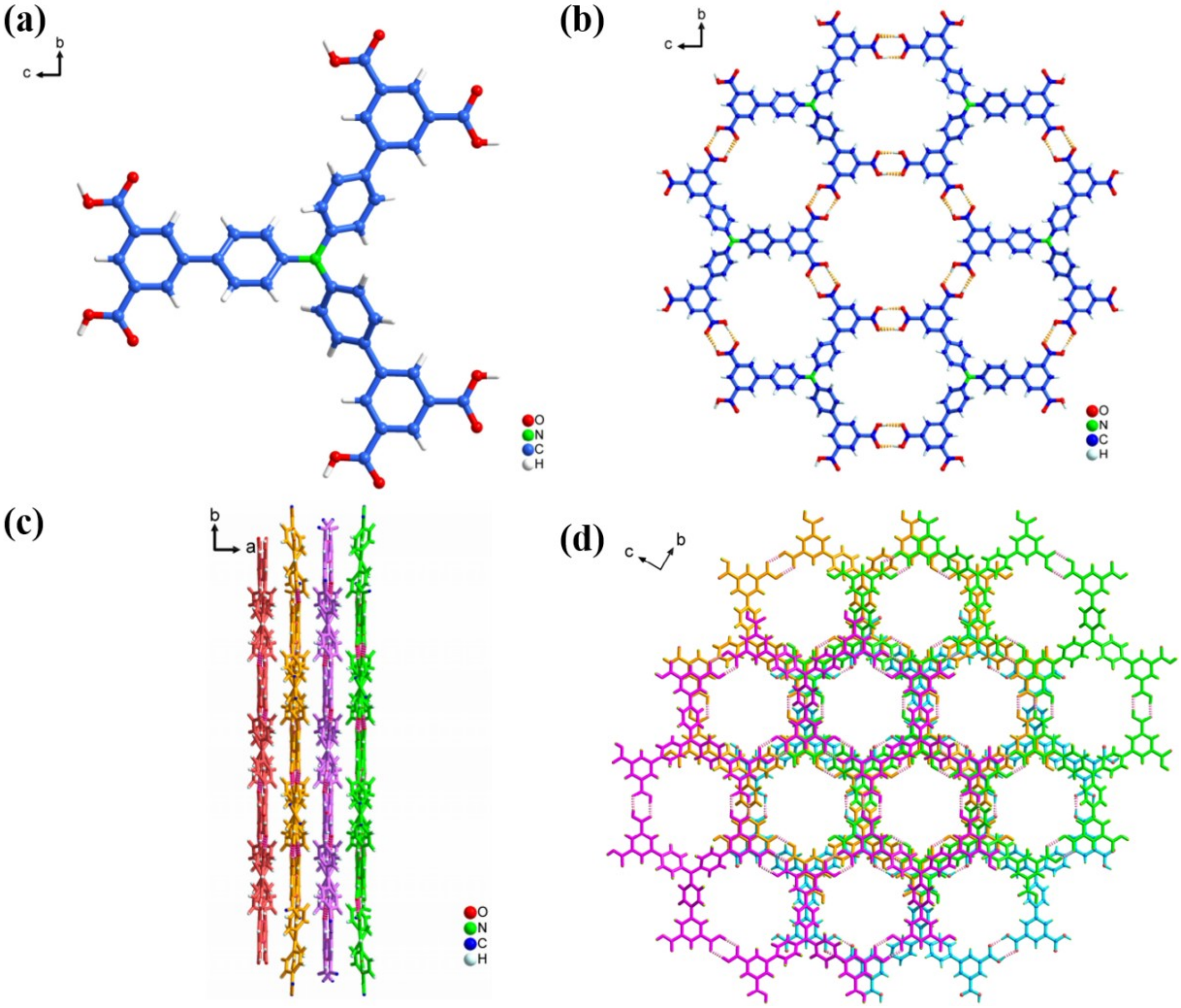

Fig. S1 (a) The molecular structure of H_6NBDA. C, blue; N, green; O, red; H, write. (b) Representation of the two kinds of hexagonal windows and the resulting monolayer network in HOF-NBDA. (c) The 1D channel of the framework seen from the *a*-axis. (d) The layered frameworks are stacked parallelly in a …ABCD… manner without interpenetration.

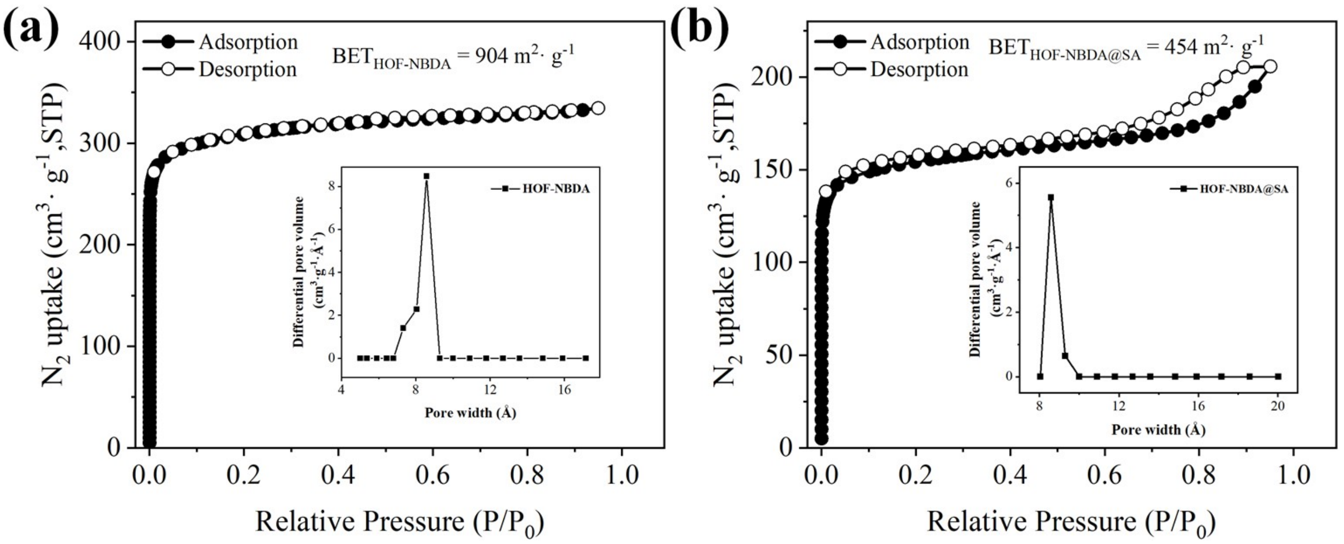

Fig. S2 N$_2$ adsorption isotherms of (a) HOF-NBDA and (b) HOF-NBDA@SA at 77 K. The inset shows the DFT pore size distribution.

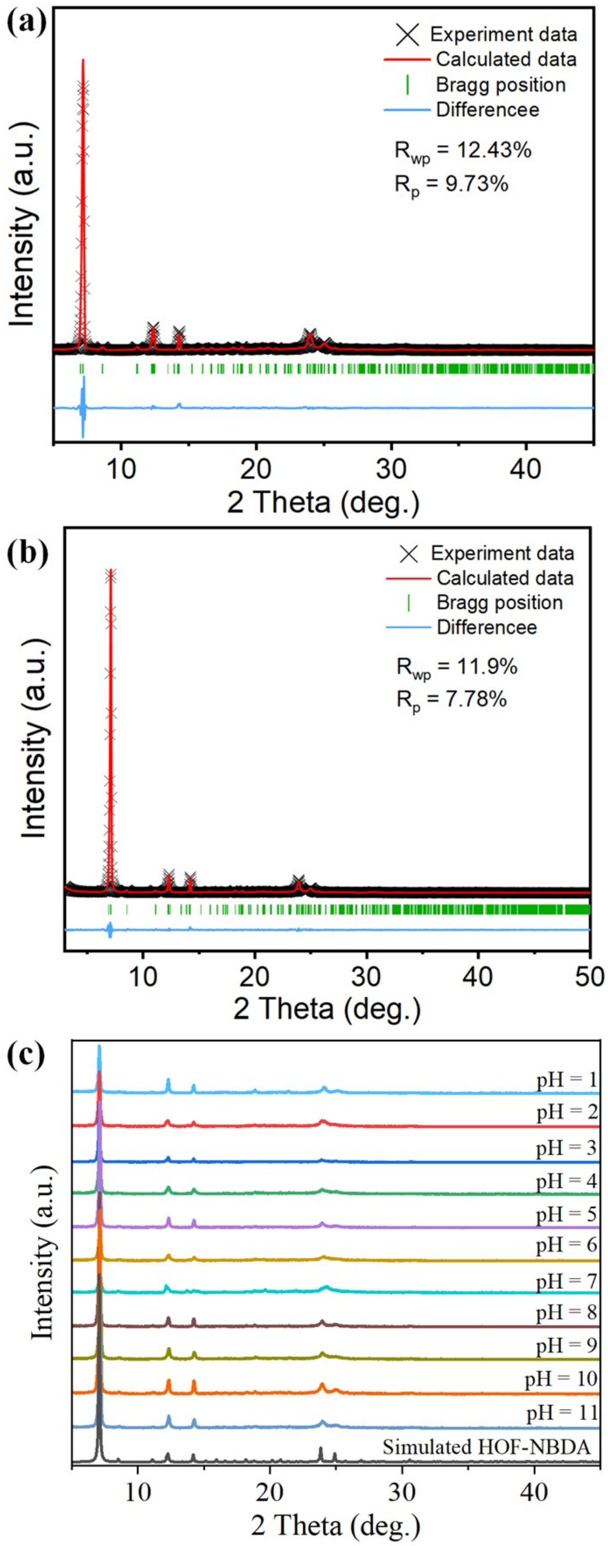

Fig. S3 (a) The refinement agreement parameters of the as-synthesized HOF-NBDA. (b) The refinement agreement parameters of HOF-NBDA after adsorption of dye. (c) PXRD patterns of HOF in 20 mL deionized water and acid-based solution (pH = 1 ~ 11) for 7 days.

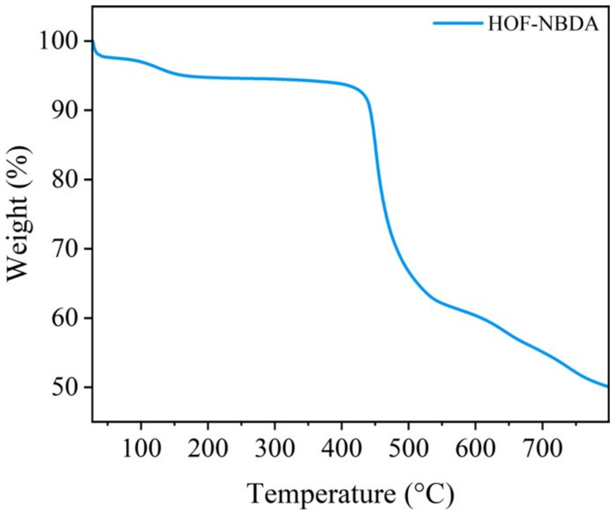

Fig. S4 TGA curve of HOF-NBDA in the nitrogen atmosphere.

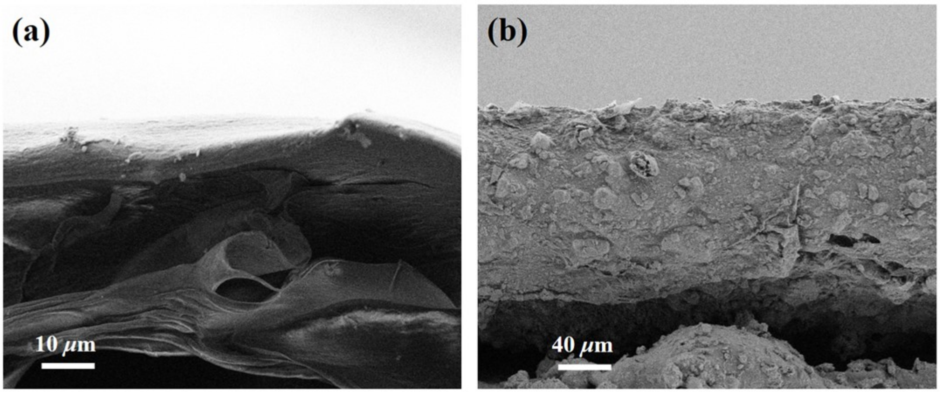

Fig. S5 The SEM images of (a) the pristine SA film and (b) HOF-NBDA@SA hydro condensate film.

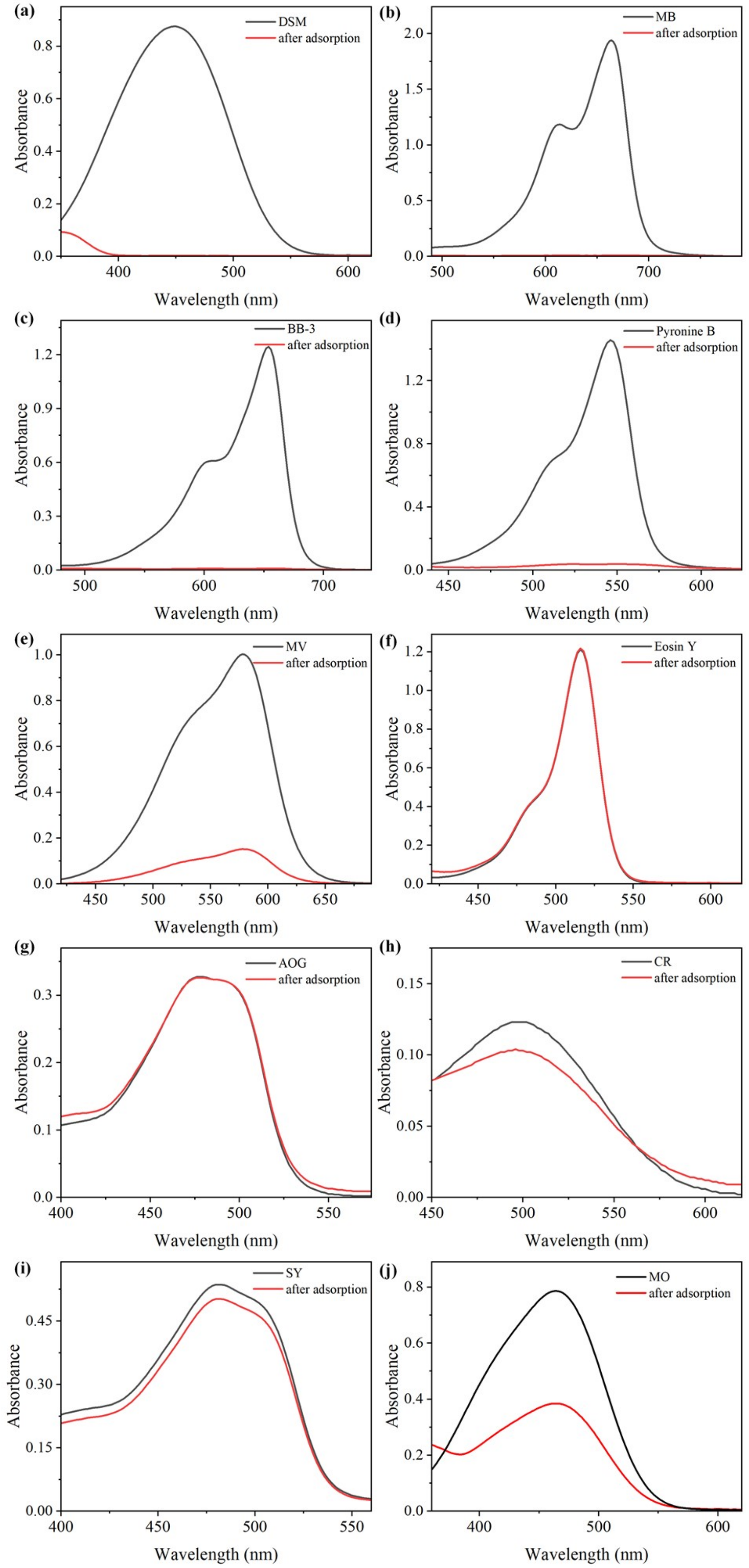

Fig. S6 Comparison of absorbance before and after adsorption of 20 ml of anion dye and cationic dye (10 ppm) at room temperature for 10 mg of HOF-NBDA for 10 min.

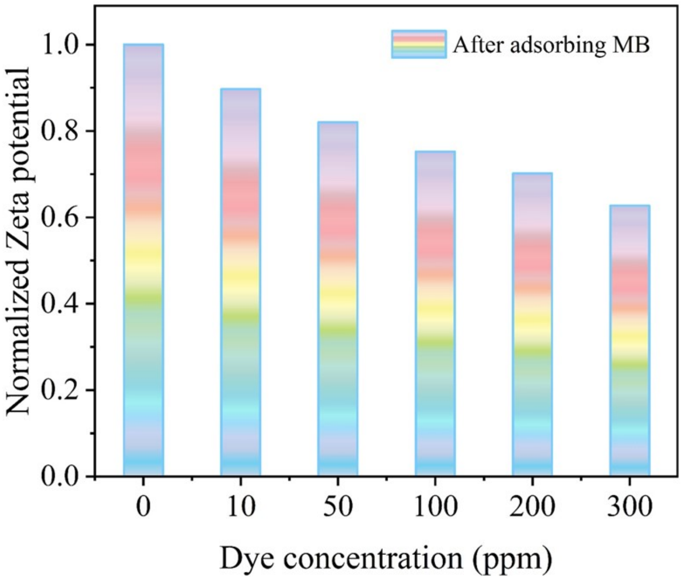

Fig. S7 The Zeta potential absolute value changes of HOF-NBDA after absorbing different concentration of MB dye.

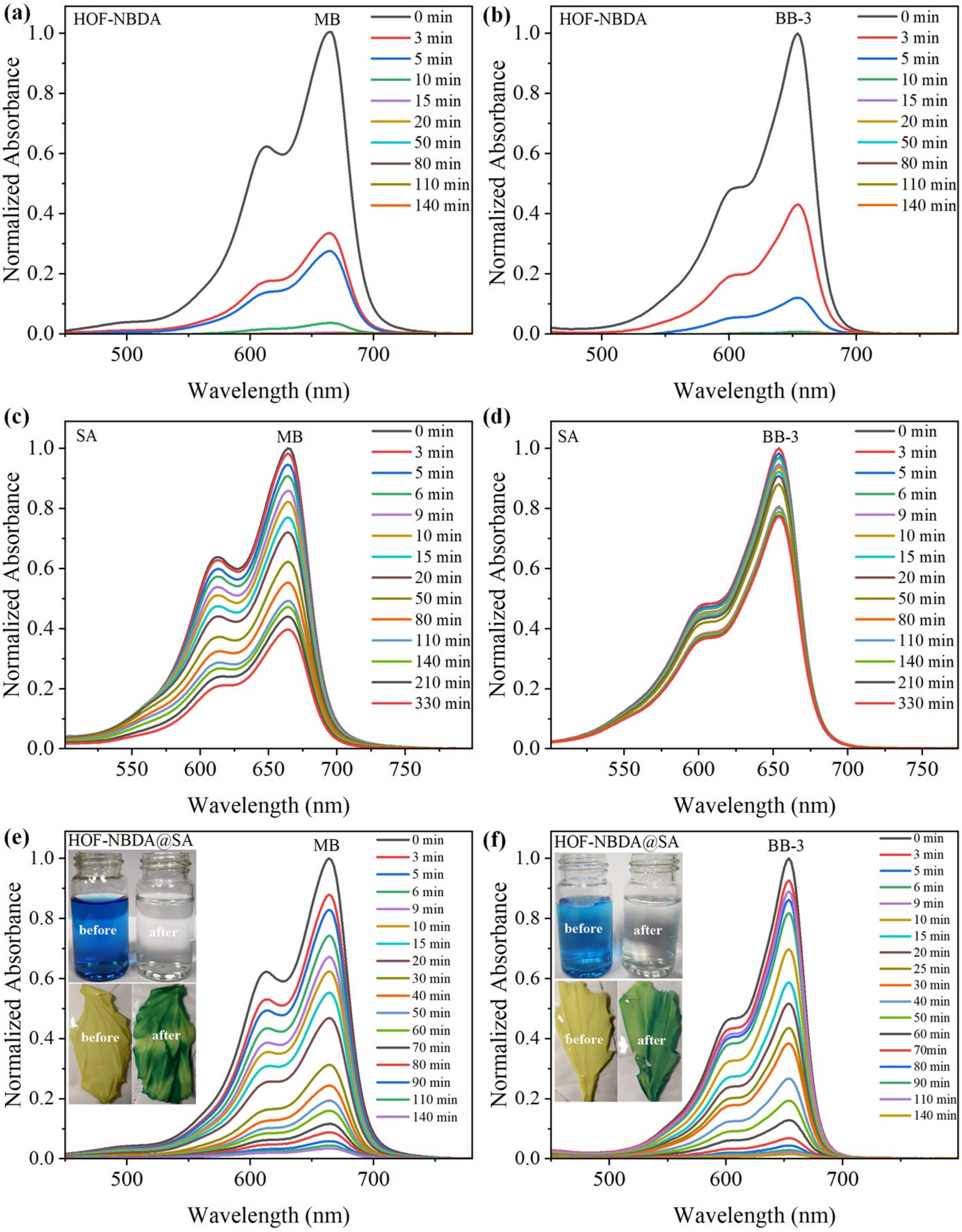

Fig. S8 (a-b) Absorbance change curves of 10 mg HOF-NBDA upon adsorption of MB and BB-3 at different times. (c-d) Absorbance change curves of 510 mg SA upon adsorption of MB and BB-3 at different times. (e-f) Change curves of absorbance of 520 mg HOF-NBDA@SA upon adsorption of MB and BB-3 at different times. In this case, both MB and BB-3 solutions varied from blue to colorless, and the corresponding membranes display the conversion from yellow to green.

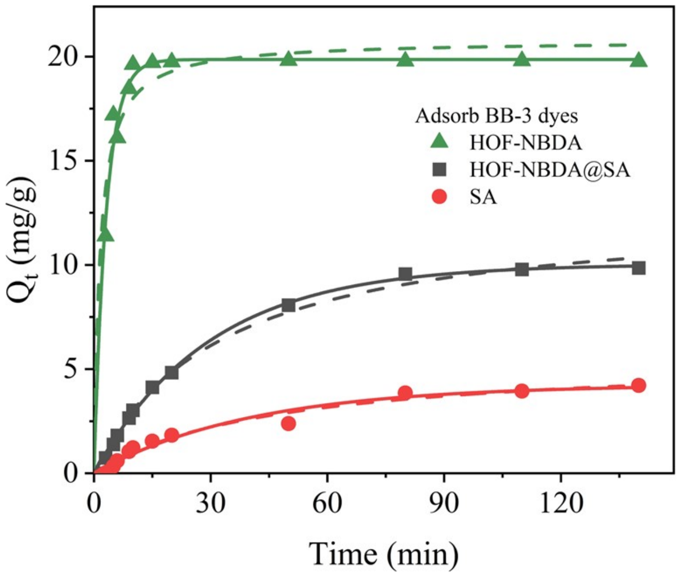

Fig. S9 Adsorption kinetics curves of 20 ml MB dye (10 ppm) adsorbed by SA, HOF-NBDA@SA and HOF-NBDA fitted to pseudo-first-order kinetic (solid line) and pseudo-second-order kinetic (dashed line) models, respectively.

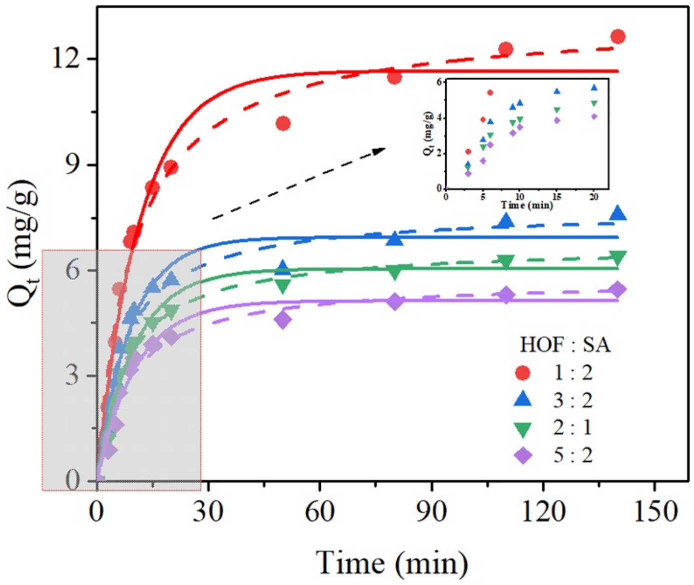

Fig. S10 Adsorption kinetics curves for adsorption of 20 ml MB dye (10 ppm) were fitted with pseudo-first-order kinetics (solid line) and pseudo-second-order kinetics (dashed line) models for the membranes with 1:2, 3:2, 2:1, and 5:2 ratios of HOF-NBDA to SA in HOF-NBDA@SA, respectively.

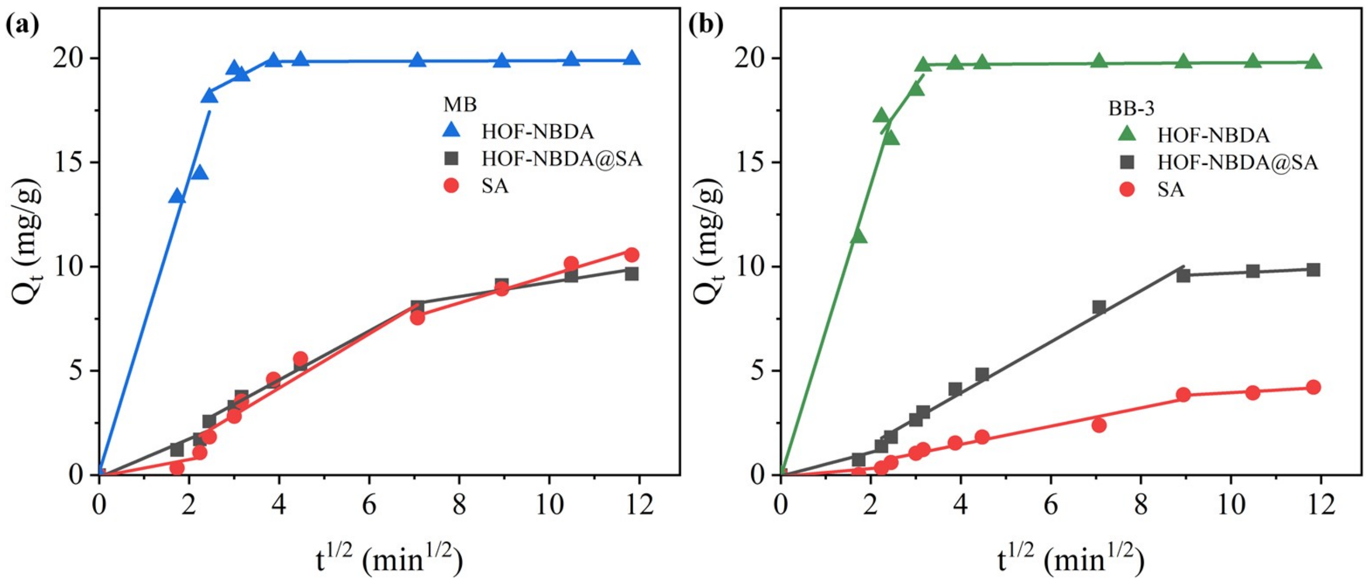

Fig. S11 Intragranular diffusion model of SA, HOF-NBDA@SA and HOF-NBDA adsorption of MB and BB-3 dyes.

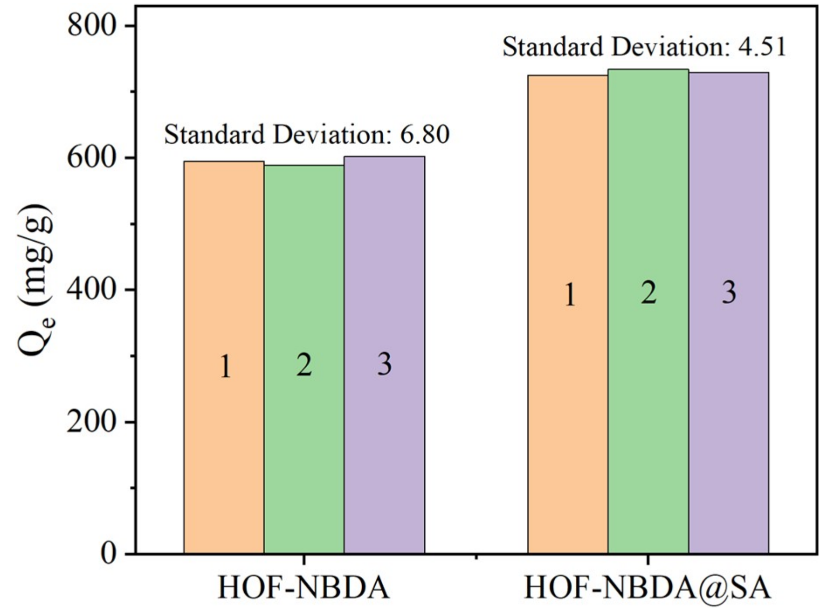

Fig. S12 The triplicate measurement of MB adsorption capacity by using HOF-NBDA and HOF-NBDA@SA obtained through three different batches of fabrication.

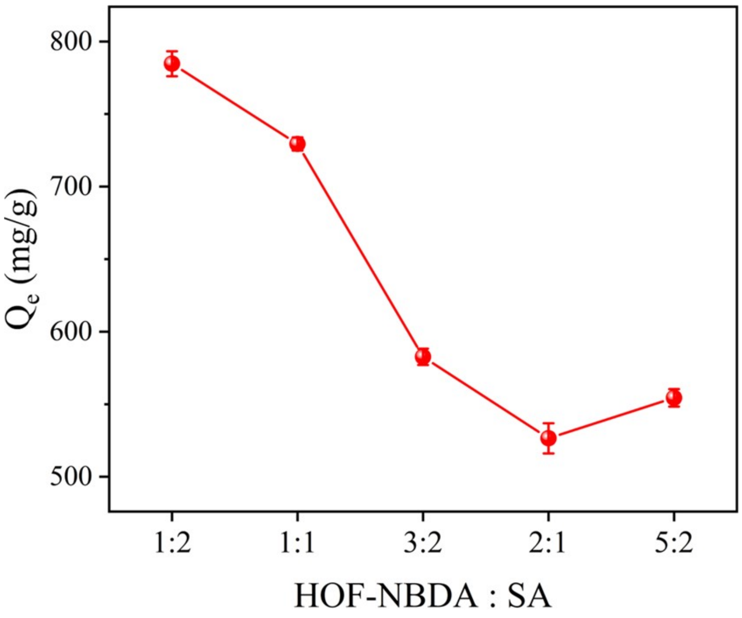

Fig. S13 The maximum adsorption capacity values of HOF-NBDA@SA membranes with different HOF-NBDA/SA weight ratios towards 20 ml MB solution (1250 ppm) when the adsorption equilibrium was reached.

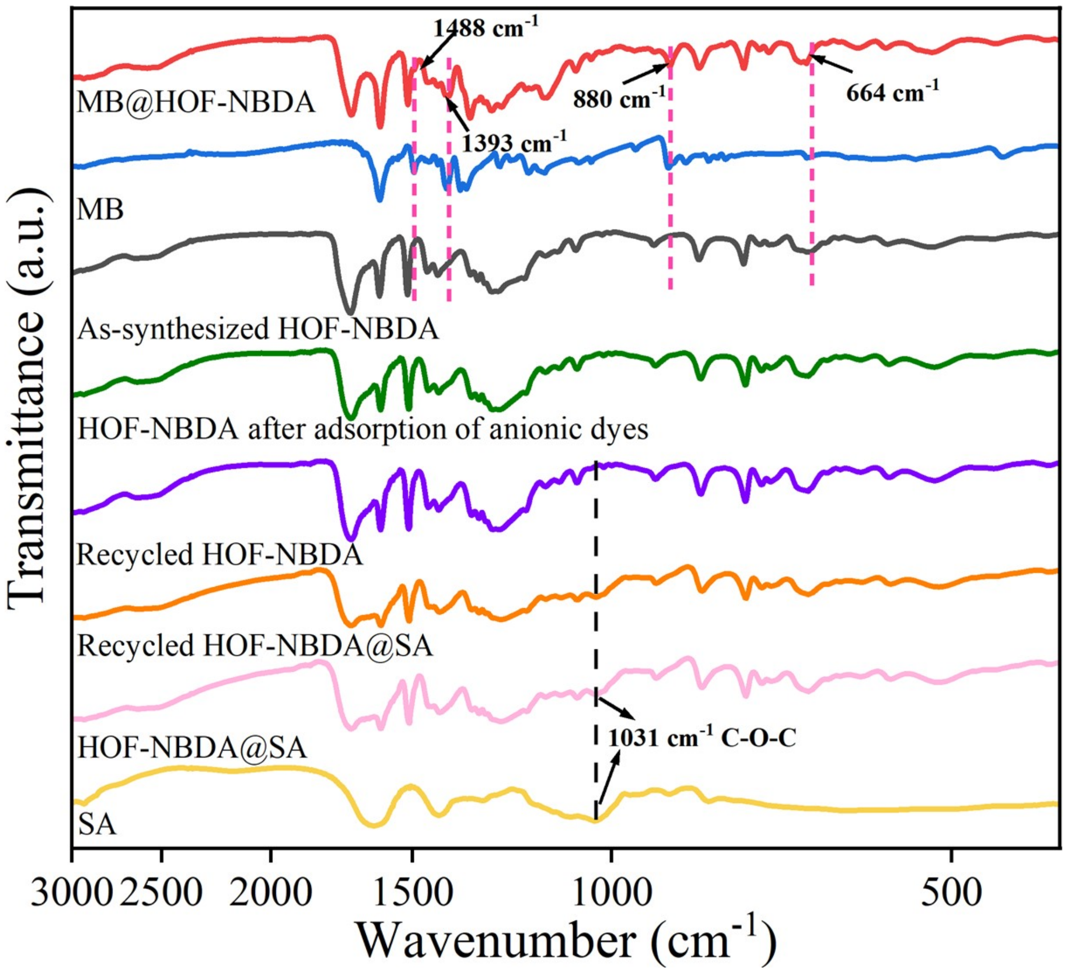

Fig. S14 FTIR spectra of MB@HOF-NBDA, MB dye, as-synthesized HOF-NBDA, HOF-NBDA after adsorption of anionic dye, HOF-NBDA and HOF-NBDA@SA after recycling, HOF-NBDA@SA and SA. In the spectrum of HOF-NBDA@SA, the peak at 1031 cm^{-1} is attributed to the C-O-C antisymmetric stretching vibration of the alicyclic ether in SA. In the spectrum of MB@HOF-NBDA, the peaks at 1488, 1393, 880, and 664 cm^{-1} are respectively attributed to –C=N absorption, –CH_3 asymmetric stretching vibration, C–H in-plane bending vibration and C–S–C skeletal vibration of MB molecule[20-22].

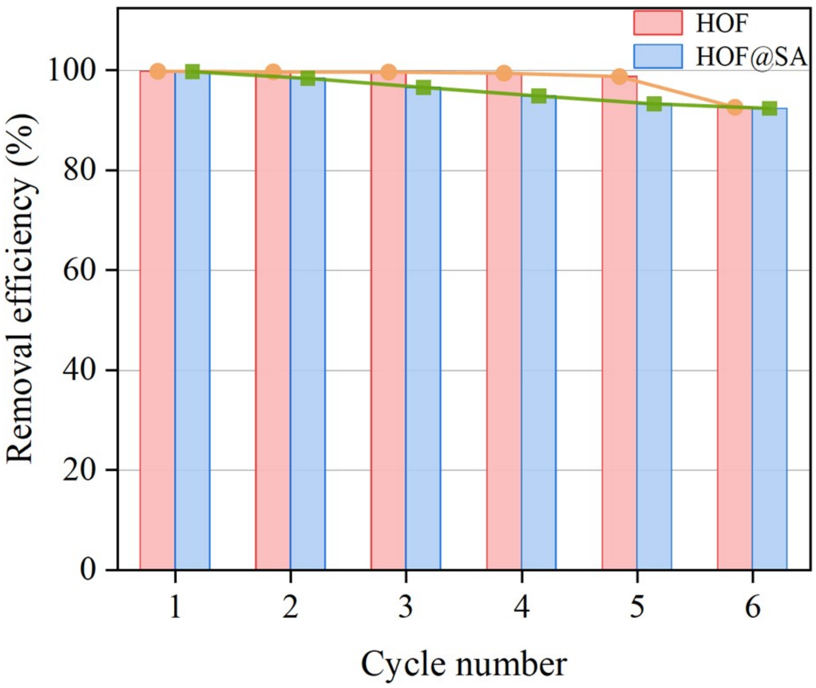

Fig. S15 Schematic diagram of the reusability of HOF-NBDA and HOF-NBDA@SA for adsorbing MB dyes.

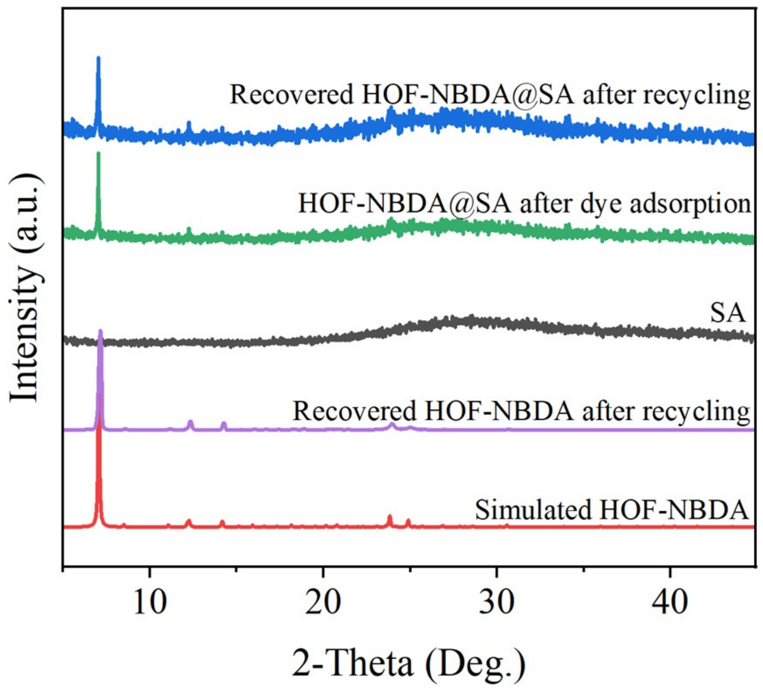

Fig. S16 PXRD patterns of simulated crystal data of HOF-NBDA, recovered HOF-NBDA after recycling, SA, HOF-NBDA@SA after adsorption of dye and recovered HOF-NBDA@SA after recycling

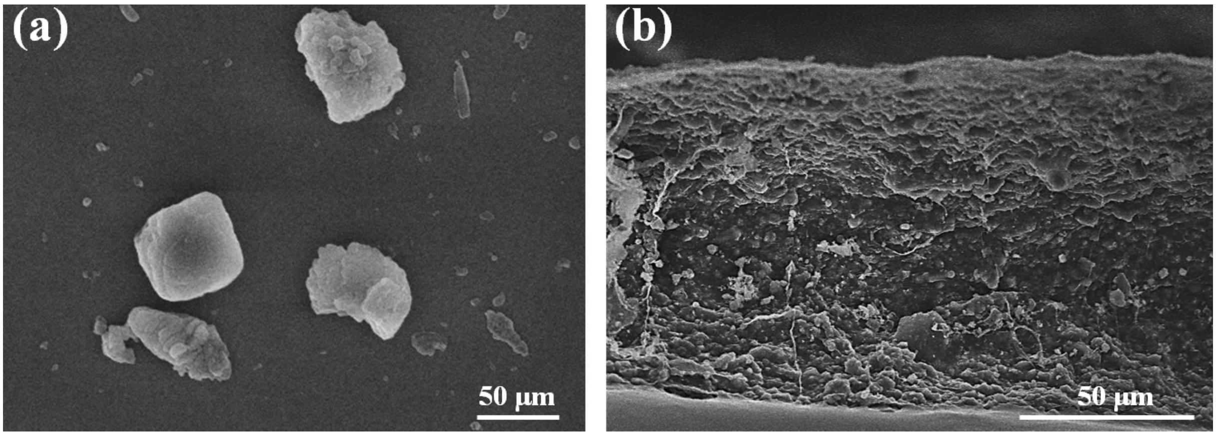

Fig. S17 The SEM images of (a) HOF-NBDA and (b) HOF-NBDA@SA film after recovery.

Reference

1 Y. Z. Zhou, C. Chen, R. Krishna, Z. Y. Ji, D. Q. Yuan and M. Y. Wu, *Angew. Chem., Int. Ed.*, 2023, **62**, e202305041.
2 G. W. Wang, Z. L. Liao, Z. W. Jiang, W. Q. Cao, Y. Yang, G. D. Qian and Y. J. Cui, *J. Mater. Chem. C*, 2023, **11**, 14551-14558.
3 A. Giri, S. Biswas, M. D. W. Hussain, T. K. Dutta and A. Patra, *ACS Appl. Mater. Interfaces*, 2022, **14**, 7369-7381.
4 D. Shetty, I. Jahovic, J. Raya, Z. Asfari, J.-C. Olsen and A. Trabolsi, *ACS Appl. Mater. Interfaces*, 2018, **10**, 2976-2981.
5 F. C. Wu, R. L. Tseng and R. S. Juang, *Chem. Eng. J.*, 2009, **153**, 1-8.
6 Z. H. Yuan, F. Li, X. F. Zhang, M. C. Li, Y. Chen, C. F. D. Hoop, J. Q. Qi and X. Y. Huang, *Environ. Res.*, 2024, **248**, 118263.
7 X. Wang, B. Cheng, L. Y. Zhang, J. G. Yu and Y. J. Li, *J. Colloid Interface Sci.*, 2022, **612**, 598-607.
8 S. Liu, J. H. Huang, W. Zhang, L. X. Shi, K. X. Yi, C. Y. Zhang, H. L. Pang, J. N. Li and S. Z. Li, *J. Hazard. Mater.*, 2022, **431**, 128643.
9 Y. H. Jin, F. Liu, Y. H. Li, Q. J. Du, F. L. Song, B. Chen, K. W. Chen, Y. Zhang, M. Z. Wang, Y. H. Sun, S. Y. Zhao, Z. Y. Jing, X. X. Pi, Y. Q. Wang and D. C. Wang, *Int. J. Biol. Macromol.*, 2023, **252**, 126198.
10 S. Kamath, J. R. Attokkaran, A. S. Maraddi, A. Samage, G. B. D'Souza, H. Yoon and S. K. Nataraj, *Chem. Eng. J.*, 2024, **479**, 147805.
11 R. Mateo del, E. Juan Carlos Grimalt, P. Gemma Turnes and C. Carlos Palomino, *Chem. Eng. J.*, 2021, **428**, 131147.
12 F. Ahmadijokani, R. Mohammadkhani, S. Ahmadipouya, A. Shokrgozar, M. Rezakazemi, H. Molavi, T. M. Aminabhavi and M. Arjmand, *Chem. Eng. J.*, 2020, **399**, 125346.
13 E. Haque, V. Lo, A. I. Minett, A. T. Harris and T. L. Church, *J. Mater. Chem. A*, 2013, DOI: 10.1039/c3ta13589f, 193.
14 C. Dai, M. Zhang, X. Guo and X. Ma, *Chem. Eng. J.*, 2020, **407**, 127181.
15 D. Tang, J. Li, Z. Yang, X. Jiang, L. Huang, X. Guo, Y. Li, J. Zhu and X. Sun, *Chem. Eng. J.*, 2021, **428**, 130954.
16 L. Yao, H. Yang, Z. Chen, M. Qiu, B. Hu and X. Wang, *Chemosphere*, 2020, **273**, 128576.
17 A. B. Albadarin, M. N. Collins, M. Naushad, S. Shirazian, G. Walker and C. Mangwandi, *Chem. Eng. J.*, 2017, **307**, 264-272.
18 T. Li, Z. Shu, J. Zhou, Y. Chen, D. Yu, X. Yuan and Y. Wang, *Appl. Clay Sci.*, 2015, **107**, 182-187.
19 L. Zhang, B. Shen, C. Zheng, Y. Huang, Y. Liang, P. Fei, J. Chen and W. Lai, *Food Hydrocolloids*, 2024, **156**, 110368.
20 H. S. Kusuma, D. E. Christa Jaya, N. Illiyanasafa, K. L. Ikawati, E. Kurniasari, H. Darmokoesoemo and A. N. Amenaghawon, *Chemosphere*, 2024, **356**, 141867.
21 D. Sarmah and N. Karak, *Carbohydr. Polym.*, 2020, **242**, 116320.
22 S. Sharma, G. Sharma, A. Kumar, T. S. AlGarni, M. Naushad, Z. A. Alothman and F. J. Stadler, *J. Hazard. Mater.*, 2022, **421**, 126729.